Nanoscale

Accepted Manuscript

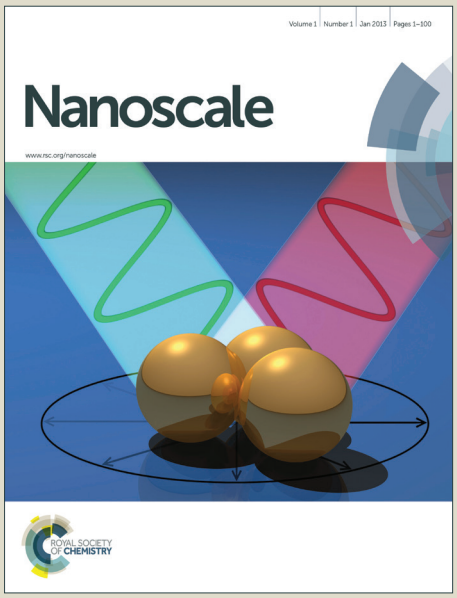

Nanoscale RSCPublishing

PAPER

Temperature-Induced Transitions of the Self-Assembled Phthalocyanine Molecular Nanoarrays at Solid-Liquid Interface: from Randomness to Order†

Cite this: DOI: 10.1039/x0xx00000x

Received 00th January 2012,
Accepted 00th January 2012

DOI: 10.1039/x0xx00000x

www.rsc.org/

Fangyun Hu,[a,b,‡] Yunnan Gong,[c,‡] Xuemei Zhang,[a] Jindong Xue,[a,b] Bo Liu,[b] Tongbu Lu,[c] Ke Deng,[a,*] Wubiao Duan,[b,*] Qingdao Zeng[a,*] and Chen Wang[a,*]

A promising approach to create functional nanoarrays is supramolecular self-assembly at liquid−solid interfaces. In the present investigation, we report on the self-assembly of phthalocyanine arrays using the triphenylene-2, 6, 10-tricarboxylic acid (H_3TTCA) as molecular nanotemplates. Five different metastable arrays are achieved in the study, including a thermodynamic stable configuration. Scanning tunneling microscopic (STM) measurements and density function theory (DFT) calculations are utilized to reveal the formation mechanism of the molecular nanoarrays. In general, the transformation process of nanoarrays is regulated by the synergies of template effect and thermodynamic balance.

Introduction

Enormous research efforts are currently devoted to molecular nanodevices, and functionalized organic molecules are promising building blocks for nanoscale electronic circuits.[1-3] Realization of this charming idea properly relies on the effective controlling the assembly of molecules into highly periodic nanoarrays on surfaces with desired functionalities. In addition, surface-supported two-dimensional (2D) monolayers are ideal model systems since their structural properities are analytically accessible by established techniques, such as scanning tunneling microscopy (STM).[4,5] In order to gain knowledge on controlling the nature of self-assembled structures by STM techniques, various approaches have been explored, including molecular designs and external stimuli.[6-16]

By rational design and synthesis of molecular building blocks, a large variety of self-assembled molecular arrays with functionality can be realized. Ultimately, molecular arrays on surfaces could be fabricated by various intermolecular interactions, including strong covalent bonding,[17-20] or cooperation of several kinds of non-covalent interactions (hydrogen bonding,[21, 22] metal-ligand coordination,[23, 24] as well as van der Waals,[25-28] *etc*.). Up till now, the following three examples are excellent achievable mastery in the field of molecular arrays. Cai *et al.* combined on-surface reaction with bottom-up method to successfully fabricate some graphene nanoribbons with atomically precise.[18] Through a spontaneous "chemical soldering" reaction, a conductive polydiacetylene nanowire was fabricated by initiating chain polymerization by stimulation with the tip.[20] Besenbacher and coworkers demonstrated that by a controlled oxidation of a Cu (110) surface as template, some well-ordered one-dimensional (1D) molecular wires of "Single Lander" molecules determined by the van der Waals interactions could form.[26]

Such reports have indicated that molecular arrays could be fabricated by rational design of molecular structures and favorable experimental methods. Nanoarrays can also be fabricated by molecular nanotemplates.[29-31] Surface confined molecular networks, especially 2D porous networks, can serve as templates to accommodate guest molecules to form molecular arrays with periodicity matching the networks.[32] Since controlled and reversible molecular manipulation is a key step in realizing future generation molecule based devices, a number of studies have focused on external stimuli. The self-assembled networks are primarily governed by the structure of the molecule,[33-37] but also can be induced by light,[38-40] concentration,[41-44]temperature,[45-48] and so on. Lei *et al.*[41] put forward a model for a transition from high density to low density phases in response to reducing concentration. Gutzler *et al.* have observed a reversible phase transformation for 1,3,5-tris(4-carboxyphenyl)benzene (BTB) from a nanoporous low-temperature phase to a more densely packed high-temperature phase at the liquid-solid interface.[46] However, no previous study has used such a transition to observe the processes for producing thermodynamically favored nanoarrays with 2D self-assembly.

Herein, we report some new-typed molecular arrays of different shapes based on the binary self-assembled system of triphenylene-2, 6, 10-tricarboxylic acid (H_3TTCA) and H_2Pc molecules at the 1-heptanoic acid–HOPG interface. The

thermodynamically favored nanoarrays of uniform shape and size can be formed by simply controlling the substrate temperature. Scanning tunneling microscopic (STM) measurements and density function theory (DFT) calculations are utilized to reveal the formation mechanism of the molecular nanoarrays.

Experimental Section

Sample preparation.

Triphenylene-2, 6, 10-tricarboxylic acid (H_3TTCA, Figure 1a) was synthesized according to the reported procedures.[49, 50] H_2Pc (98%, Figure 1b) was purchased from TCI Company, and used without any further purification.

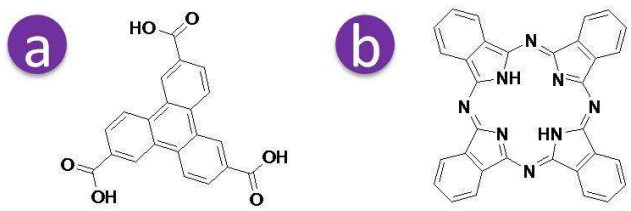

Figure 1. Chemical structures of (a) H_3TTCA, and (b) H_2Pc.

In all the experiments, highly oriented pyrolytic graphite (HOPG, ZYB, NT-MDT, Russia) substrates were used. For STM imaging, saturated solutions of the H_3TTCA and H_2Pc were prepared by dissolving approximately 1.0 mg of solid per 2 mL of 1-heptanoic acid, respectively. To aid in solubilizing, the solution was put in an ultrasonic bath for approximately 10 min. After the sonication, the solutions were left unperturbed to equilibrate for an overnight prior to deposition for imaging. The typical concentrations of the saturated solutions were ~ 10^{-3} M.

STM investigation.

STM measurements were performed by using a Nanoscope IIIa (Bruker, USA) under ambient conditions. All STM images presented were recorded in constant current mode using different kinds of mechanically cut Pt/Ir (80/20) tips. The thermal drift was corrected using the underlying graphite lattice as a reference. The latter lattice was visualized by lowering the bias voltage to 50 mV and raising the current to 800 pA during image acquisition. And the "error values" on the lattice parameters were obtained by the statistical method. The specific tunneling conditions were given in the corresponding figure captions.

Normally, a droplet (5 μL) of the 1-heptanoic acid solution containing H_3TTCA, was first deposited onto a freshly cleaved surface (5×5 mm^2) of HOPG. A few minutes later, the sample was then studied. To accomplish the incorporation of the guests, a droplet (5 μL) of solution containing H_2Pc was then added on top of the studied sample. After 10 minutes, the STM investigation was performed. The mole ratio was controlled by both the concentration and volume deposited. And all the experiments were repeated at least five times. The structure of the assembly was investigated by STM with the tip immersed in the liquid. 1-Heptanoic acid is electrically nonconductive, and its vapor pressure at room temperature is low enough to allow for stable tunneling experiments.

Computational details

We have performed theoretical calculations using DFT provided by DMol3 code.[51] The Perdew and Wang parameterization[52] of the local exchange correlation energy was applied in local spin density approximation (LSDA) to describe exchange and correlation. We expanded the all-electron spin-unrestricted Kohn–Sham wave functions in a local atomic orbital basis. For the large system, the numerical basis set was applied. All calculations were all-electron ones, and performed with the medium mesh. Self-consistent field procedure was done with a convergence criterion of 10^{-5} au on the energy and electron density.

Results and Discussion

H_3TTCA: Assembly Honeycomb Network Structures of Host Molecules

The structure of H_3TTCA is depicted in Figure 1a and can be regarded as a central triphenylene which is symmetrically substituted with three carboxylic acid groups in 3-fold symmetrical manners. The H_3TTCA is a planar molecule, allowing for the spontaneous formation of supramolecular architectures via directed hydrogen bonding to neighboring molecules on surfaces.

The self-assembled structures are initiated by depositing a droplet of H_3TTCA solution onto a freshly cleaved HOPG surface and verified by STM at the liquid-solid interface. For 100% saturation, the densely packed row structure with striped appearance is a dominated structure at the 1-heptanoic acid–HOPG (Figure S1). At a concentration of 50% saturation, a network structure starts to appear on the surface, yet in coexistence with the densely packed row structure on the surface (Figure S2). At concentrations around 10% and even 1% of saturation, the network structure is exclusively formed, which is shown in Figure 2a. And around 1% saturation, a considerably unstable self-assembled monolayer is even captured (Figure S3). It indicates that at this low concentration, the number of dissolved molecules in the liquid phase is already comparable to the number of molecules in the monolayer. A clear correlation between solute concentration and dominance of one of the monolayer phases has been found: the lower the concentration of solution is, the lower the packing density of molecules on the surface is.

The polymorph emphasizes the importance of solute concentration in H_3TTCA molecular self-assembly at the 1-heptanoic acid–HOPG. So the formation of network structure can be easily achieved by controlling the concentrations around 10% to even 1% of saturated solution. After heating the above-mentioned chicken-wire structure at temperatures up to ~333 K for about 10 minutes, no phase transition of the monolayer morphology is observable. At all intermediate temperatures, the chicken-wire structure is exclusively observed. Therefore, it points out that even after heating to ~333 K, the network structure appears to be thermodynamically stable. However, for some other 3-fold symmetric tricarboxylic acids, like 1,3,5-tris (4-carboxyphenyl) benzene (BTB), the interfacial monolayers show a fully reversible temperature-driven structural phase transition, changing from the chicken-wire structure to a nonporous densely packed structure.[46]

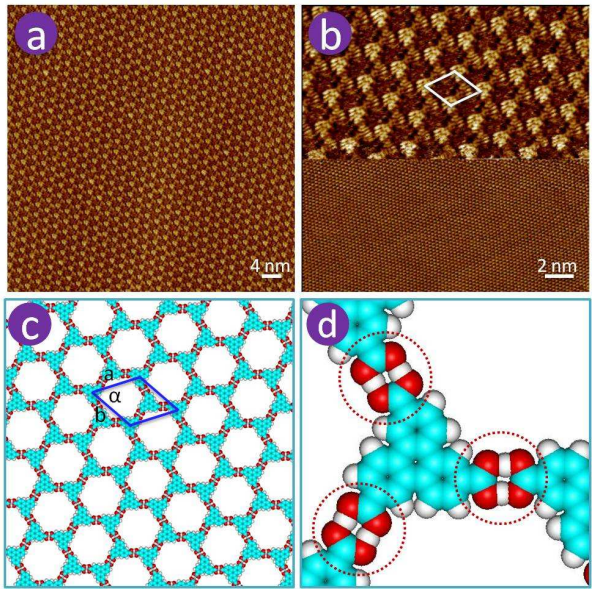

Figure 2. STM images of the assembling chicken-wire structures of H_3TTCA. (a) A typical large scale STM image of H_3TTCA assembled chicken-wire structure under the chosen experimental conditions (at room temperature, and 1% saturated solution). I = 296.0 pA, V = 594.9 mV. (b) A composite High-resolution STM image of chicken-wire structure (the upper part) and HOPG substrate (the lower part). By lowering the bias voltage during scanning, the underlying graphite surface can be imaged simultaneously. Imaging conditions: I = 297.5 pA, V = 625.4 mV (the upper part); I = 800.0 pA, V = 50.0mV (the lower part). (c), (d) are suggested molecular models for the observed area in (a).

Then, under the chosen experimental conditions (at room temperature, and 1% saturated solution of H_3TTCA in 1-heptanoic acid), the large-area honeycomb network structures demonstrated in Figure 2a can be realized easily. The H_3TTCA formed topologically honeycomb networks, which is also quite common for other 3-fold symmetrical tricarboxylic acids, like trimesic acid (TMA) on HOPG surfaces.[53, 54] This porous arrangement of H_3TTCA, is composed of the acid molecules with perfect arrangement of the hydrogen bonds. A typically high-resolution STM image is presented in Figure 2b, within a single frame both the adsorbate layer and the substrate are recorded with molecular and atomic resolution, respectively. A single H_3TTCA molecule appears as three clearly separated protrusions in a 3-fold arrangement. Careful analysis of the submolecular structure of single H_3TTCA molecule reveals that each of the three carboxylic groups per molecule forms two hydrogen bonds with its neighbors (see the red dashed circles Figure 2d). Every molecule is part of three neighboring rings, and is interconnected by linear double O-H ··· O hydrogen bonds between carboxylic groups. According to the STM image, a corresponding molecular model was proposed in Fig. 2c. The measured unit cell parameters are: a = b = 2.3 ± 0.1 nm and α = 60 ± 1°, which agrees well with the expected size by density functional theory (DFT) calculation (a = b = 2.39 nm, α = 60°). The hydrogen bonding between a H_3TTCA dimer is about - 44.35 kcal·mol^{-1}. And the total energy (including the interaction between adsorbates, and the interaction between adsorbates and substrate) per unit area is - 0.332 kcal·mol^{-1}·Å^{-2}. Here, the more negative energy means the system is more stable.

The above-mentioned observations can be taken as an indication that H_3TTCA forms porous and topologically chicken-wire structure in the chosen experimental conditions, which can be quite thermodynamic stable. And considering that the formed chicken-wire network is linked together just by the hydrogen bonds between the -COOH, the possible rearrangement of the networks would lead to the inclusion of functional guest molecules. It was also shown in previous study that chicken-wire structure may act as a template for TMA itself because the size of one TMA molecule fairly fitted the cavity size.[55] However, in our experiment, the H_3TTCA molecules within the cavity appears rather faint when compared with the TMA-formed chicken-wire structures. So the chicken-wire structure is perhaps an adjustable template for other guest molecules.

H_2Pc @H_3TTCA: Five Kinds of Molecular Nanoarrays

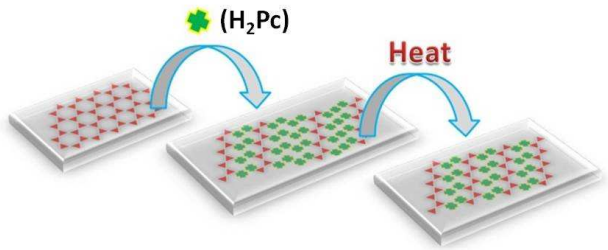

Scheme 1. Hierarchical self-assembled procedures and temperature-induced transformations.

The bottom-up method of increasing diversity and functionality relies on hierarchic assembled steps, where each step progressively sets the base for the next.[56-60] As illustrated in the Scheme 1, a two-step process happens in our study. We first induce a thermodynamic stable template, add guest molecules to form nanoarrays and then control the morphologies of nanoarrays. The chosen guest molecular structure is shown in Figure 1b, H_2Pc is a planar molecule without any function groups. It does not geometrically match well with H_3TTCA pores, as H_2Pc is not a 3-fold symmetrical manner as H_3TTCA, but a 2-fold symmetrical manner. Owing to these reasons, H_2Pc molecules may break the H_3TTCA-formed chicken-wire structures.

Once the STM is driftstable and a submolecular resolution of the host network is obtained, an additional droplet of solution containing the guest molecule H_2Pc is added. The regular H_2Pc@H_3TTCA arrays are observed by STM immediately after injection. In the typically large-area STM images (Figures S4, S5), the perfect arrangement of the guest molecules within the H_3TTCA bearings are demonstrated. Interestingly, the originally chicken-wire structure is broken, and considering the concentration of H_3TTCA is even more diluted as more solvent comes from H_2Pc solution, this new structure is supposed not dominated by the concentration of H_3TTCA anymore. The hydrogen bonds between carboxyl groups are very strong, it is a bit surprising to see H_2Pc can break H3TTCA hydrogen bonds and inserted into the H_3TTCA arrays. Also in nH_2Pc@H_3TTCA arrays, like the 2H_2Pc@H_3TTCA , H_2Pc molecules only interacte with each other, but the distance between the neighboring dimer is much larger than the intermolecular distance in the dimer. This means the H_2Pc arrays are only stabilized by the weak hydrogen bonds with H_3TTCA and van der Waals interactions between dimers in one direction, while on the other direction, no significant interaction stabilizes them.

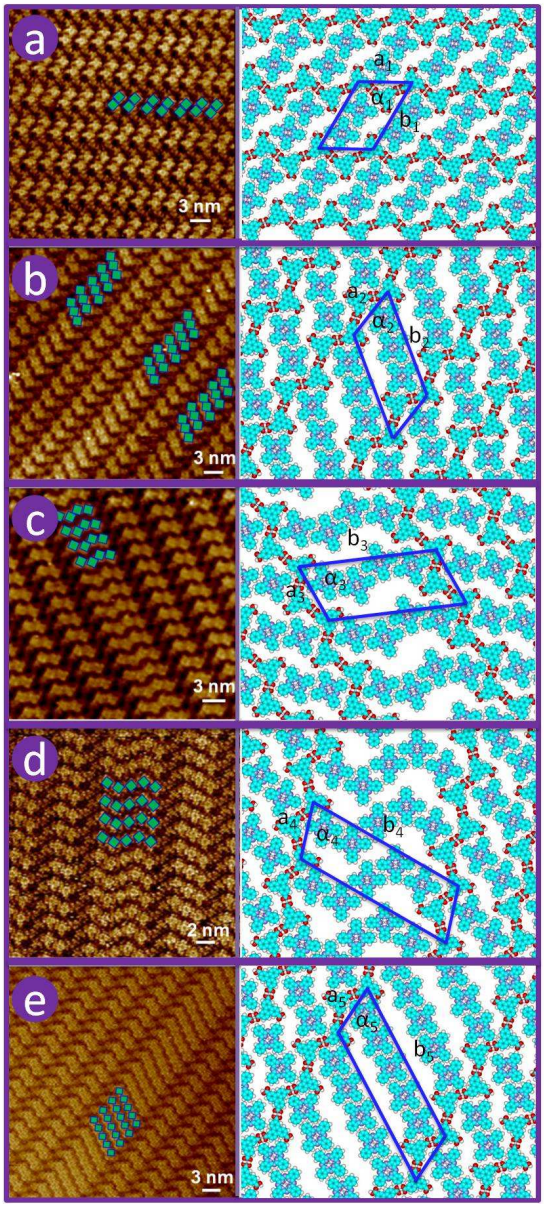

Figure 3. An overview of the random arrays which are immobilized in the rearrangement H_3TTCA networks for the H_2Pc@H_3TTCA system. While for the 3H_2Pc@H_3TTCA, 4H_2Pc-zigzag@H_3TTCA, 5H_2Pc-line@H_3TTCA or 5H_2Pc-zigzag@H_3TTCA, they merely occur as one array surrounded by 2H_2Pc@H_3TTCA. On the left hand side, high-resolution STM images of all the five kinds of nanoarrays are shown for the H_2Pc@H_3TTCA system at the 1-heptanoic acid/HOPG interface, H_2Pc molecules are indicated by the blue squares. I = 405.9 pA, V = 692.1 mV. Schematic corresponding molecular models of all assemblies are presented on the right side. The concentrations of all the solutions used are less than 10^{-3} M, and H_3TTCA: H_2Pc = 1:1.

Occasionally-occurring point defects in the images are also observed due to vacancy of H_2Pc molecules. It is possible to routinely reproduce this coadsorption experiment. And only five distinct kinds of long nanoarrays formed by H_2Pc, namely 2H_2Pc@H_3TTCA (the basic unit of nanoarray consisting of a H_2Pc-formed dimer and two H_3TTCA), 3H_2Pc @H_3TTCA (the trimer of H_2Pc and two H_3TTCA), 4H_2Pc-zigzag@H_3TTCA (the zigzag-shaped tetramer of H_2Pc and two H_3TTCA), 5H_2Pc-zigzag@H_3TTCA, and 5H_2Pc-line@H_3TTCA are observed (see Figure 3). The bright spots (highlighted with the blue squares) can be ascribed to H_2Pc molecules.

The high-resolution STM images emphasize the local molecular arrangements of the five kinds of assembled structures, which are almost in the same manner. Here the triangular feature represents a single H_3TTCA and the four-lobe feature corresponds to a single H_2Pc molecule, respectively. Both H_3TTCA and H_2Pc molecules lie flat on HOPG with their conjugated π-plane oriented parallel to the HOPG surface due to interfacial π–π interactions. In the molecular models, the H_3TTCA molecules assemble into zigzag molecular rows through intermolecular hydrogen bonds between carboxyl groups along one direction. And each H_3TTCA host molecule leaves one carboxyl group to "grasp" H_2Pc molecules, mainly through intermolecular hydrogen bonds between carboxyl groups and the peripheral phenyl of H_2Pc. Meanwhile, the template effects of H_3TTCA contribute to "grasp" more other H_2Pc. And considering that the interaction between H_2Pc molecules is dominated by relatively weak and non-directional van der Waals force, the H_2Pc-formed arrays have different shape, such as zigzag and line. An interesting phenomenon in the case of tetramers, only zig-zag arrays are formed, while both linear and zigzag arrays exist for H2Pc pentamers.

We also investigate the H_2Pc@H_3TTCA systems in terms of molecular ratio and concentrations of molecules. We find the organization of H_2Pc arrays on the HOPG surface is random. We do not obtain any orderly structure of 3H_2Pc@H_3TTCA, 4H_2Pc-zigzag@H_3TTCA, 5H_2Pc-line@H_3TTCA or 5H_2Pc-zigzag@H_3TTCA like the 2H_2Pc@H_3TTCA structure. In our experiments, the regular patterns of 2H_2Pc@H_3TTCA arrays are recorded mostly. While for 3H_2Pc@H_3TTCA, 4H_2Pc-zigzag@H_3TTCA, 5H_2Pc-line@H_3TTCA or 5H_2Pc-zigzag@H_3TTCA, they merely occur as one array surrounded by 2H_2Pc@H_3TTCA network. This phenomenon indicated that 4H_2Pc-zigzag@H_3TTCA, 5H_2Pc-line@H_3TTCA, 5H_2Pc-zigzag@H_3TTCA and 3H_2Pc@H_3TTCA maybe not the thermodynamically stable structures. And 2H_2Pc@H_3TTCA is the most stable in our system. In our experiment, we do not get more than pentamer-shaped H_2Pc arrays even with our effort.

The all corresponding unit cells of the five self-assembled arrays are superimposed on the right of Figure 3. And the detailed lattice parameters for the five types of H_2Pc self-assembled nanoarrays are shown in the Table 1.

Five Kinds of Nanoarrays Change into an Exclusive Order Array: Thermodynamic Controlled

The ability to visualize dynamic processes and control metastable states is very invaluable. Based on the above-mentioned experimental phenomena, a law can be easily found: The 2H_2Pc@H_3TTCA occurs most frequently, and other kinds of arrays are always randomly surrounded by 2H_2Pc@H_3TTCA. This means that the 2H_2Pc@H_3TTCA may be the most stable array in all five kinds of nanoarrays. Owing to the noncovalent interactions involved in the self-assembly process at the liquid-solid interface, the optimum conditions can be achieved to form the thermodynamically stable structures after annealing.

To investigate the temperature-controlled structural transformation, *ex situ* STM experiments are performed to investigate the change of the seemingly disordered nanoarrays into the long-range ordered structure. We found that after the samples were annealed at ~323 K for 10 minutes, the nanoarrays became ordered. In the chosen experimental condition, a large-scale structure without any defect can be realized easily, the nearly close-packed array of 2H_2Pc@H_3TTCA structure is shown in Figure 4a. Some typically high-resolution STM images are presented in Figure 4b and Figure

S6, where the H_3TTCA molecules assemble into zigzag molecular rows through intermolecular hydrogen bonds between carboxyl groups along one direction and each H_3TTCA host molecule leaves one carboxyl group to "grasp" H_2Pc molecules through intermolecular hydrogen bonds between carboxyl groups and the peripheral phenyl of H_2Pc. According to the STM observations, a supposed molecular model is provided with a unit cell superimposed: $a_6 = 2.3 \pm 0.1$ nm, $b_6 = 3.4 \pm 0.1$ nm and $\alpha_6 = 60 \pm 2°$.

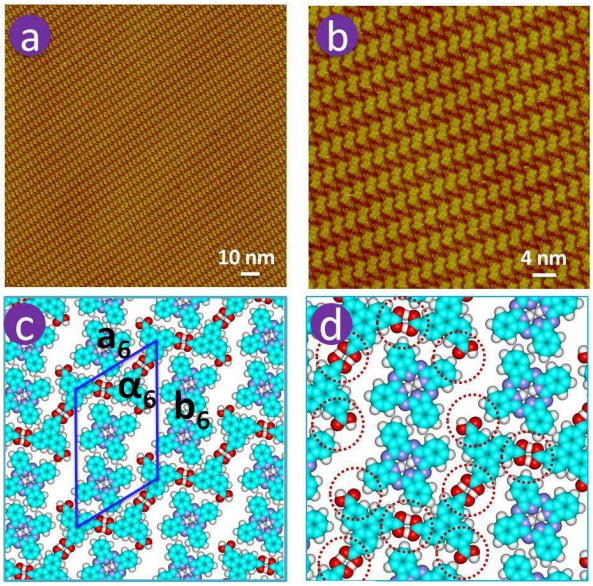

Figure 4. STM images of the ordered molecular arrays for the $H_2Pc@H_3TTCA$ binary system after the samples were annealed at ~323 K for 10 minutes. (a) A large scale STM image of $2H_2Pc@H_3TTCA$ array structures under the chosen experimental conditions, I = 380.9 pA, V = 600.1 mV. (b) A high resolution STM image of ordered $2H_2Pc@H_3TTCA$ array structures, I = 380.9 pA, V = 600.1 mV. (c) A tentative model for the observed area in (b) and a unit cell is superimposed on it. The hydrogen bonds which could be clearly distinguished by the red dashed circles in (d).

Based on these observed phenomena, the density functional theory (DFT) calculations have been performed to further investigate the target-molecule self-assembled structures on HOPG.

Table 1. Experimental (Expt.), calculated (Cal.) lattice parameters for the five types of H_2Pc self-assembled 1D nanoarrays and yet unobserved structure.

		unit cell parameters		
		a (nm)	b (nm)	α (°)
$2H_2Pc@H_3TTCA$	Expt.	2.3 ± 0.1	3.4 ± 0.1	60 ±2
	Cat.	2.38	3.45	60
$3H_2Pc@H_3TTCA$	Expt.	2.3 ± 0.1	4.5 ± 0.1	60 ±2
	Cat.	2.38	4.60	60
$4H_2Pc$-zigzag$@H_3TTCA$	Expt.	2.3 ± 0.1	5.5 ± 0.1	69 ±2
	Cat.	2.38	5.50	70
$4H_2Pc$-line$@H_3TTCA$	Expt.	--	--	--
	Cat.	2.38	6.30	60
$5H_2Pc$-zigzag$@H_3TTCA$	Expt.	2.3 ± 0.1	6.9 ± 0.1	69 ±2
	Cat.	2.38	6.70	70
$5H_2Pc$-line$@H_3TTCA$	Expt.	2.3 ± 0.1	6.8 ± 0.1	59 ±2
	Cat.	2.38	7.0	60

The calculated lattice parameters for the 1D nanoarrays are summarized in Table 1. It is clear that the calculated parameters of the theoretical models agree well with the experimental values. Furthermore, we calculate the total energy and total energy per unit area for $nH_2Pc@H_3TTCA$ arrays as shown in Table 2. The total energy includes the interactions between adsorbates (H_3TTCA and H_2Pc molecules), and the interactions between adsorbates and graphite. Therefore, we can compare thermodynamic stability of the different arrays by the total energy per unit area. Although the total energy decreases with the increase of number of H_2Pc in the array, the total energy per unit area of $nH_2Pc@H_3TTCA$ (n = 2, 3, 4, or 5) increases.

The total energy per unit area of $2H_2Pc@H_3TTCA$ is the lowest (-0.357 $kcal{\cdot}mol^{-1}{\cdot}Å^{-2}$), which is much lower than that of the pure H_3TTCA network (-0.332 $kcal{\cdot}mol^{-1}{\cdot}Å^{-2}$). Therefore, when H_2Pc molecules are added in the system, the $2H_2Pc@H_3TTCA$ structure is the thermodynamically favorable, and instead of the original H_3TTCA network. It agrees well with our experiments, in which generally, the $2H_2Pc@H_3TTCA$ network is recorded after the samples are annealed. We also notice that the total energy per unit area of $3H_2Pc@H_3TTCA$ is -0.326 $kcal{\cdot}mol^{-1}{\cdot}Å^{-2}$. Subsequently, as the less stable structure, some $3H_2Pc@H_3TTCA$ patterns often occur in the large scale $2H_2Pc@H_3TTCA$ network. The $4H_2Pc@H_3TTCA$ and $5H_2Pc@H_3TTCA$ arrays are with the higher total energy per unit area. Accordingly, they can be recorded by STM occasionally. Evidently, the $4H_2Pc$-line$@H_3TTCA$ is with the highest total energy per unit area, which means such structure is thermodynamically unstable. And we could not observe $4H_2Pc$-line$@H_3TTCA$ array in our experiment.

Table 2. Total energies (E_{total}), and total energy per unit area for the observed 1D nanoarrays and yet unobserved structure. The total energy includes the interaction between adsorbates (H_3TTCA and the guest H_2Pc molecules) and the interaction between adsorbates and graphite. Here, the more negative energy means the system is more stable.

	Total energy (E_{total}, $kcal{\cdot}mol^{-1}$)	Total energy per unit area (E_{total}, $kcal{\cdot}mol^{-1}{\cdot}Å^{-2}$)
H_2Pc-netwok	-164.287	-0.332
$2H_2Pc@H_3TTCA$	-255.158	-0.357
$3H_2Pc@H_3TTCA$	-310.254	-0.326
$4H_2Pc$-zigzag$@H_3TTCA$	-356.516	-0.289
$4H_2Pc$-line$@H_3TTCA$	-346.686	-0.266
$5H_2Pc$-zigzag$@H_3TTCA$	-413.627	-0.275
$5H_2Pc$-line$@H_3TTCA$	-405.510	-0.280

The observation of polymorphism driven only by heating identity in this relatively simple system is quite interesting. On the basis of the theoretical simulations, it is revealed that the formation of molecular arrays is attributed to the rearrangement of 2D H_3TTCA chicken-wire network by the inclusion of H_2Pc molecules. Furthermore, the structural changes initiated by heating of the binary self-assembled $H_2Pc@H_3TTCA$ array structures prove that the adsorbed monolayers are in thermodynamically metastable state at the liquid-solid interface. And the thermodynamically stable structures ($2H_2Pc@H_3TTCA$) can be achieved after annealing and consequently form thermodynamical equilibrium. The metastable state is the virtue intermediate state for the formation of complex structures. Generally, polymorphism arises when one "crystalline" form of a species is more thermodynamically stable than the other, whereas the less stable form is kinetically favored. Under the right conditions, the less stable moiety will form first but ultimately reverts to the more stable polymorph.

It is noteworthy that investigations of H_2Pc at the liquid-solid interface in 1-heptanoic acid without the H_3TTCA host molecule did not show any ordered structures for the best of our effort. This is indicative of the fact that the H_3TTCA network serves as a molecular bearing which can stabilize and enable the H_2Pc adsorption from solution. The binary solution of H_3TTCA and H_2Pc leads to a co-adsorbed monolayer just in a few seconds at room temperature. And only $2H_2Pc@H_3TTCA$ structures occur with the deformed H3TTCA networks (see Figure S7). This indicates that both H_3TTCA and H_2Pc molecules are adsorbed simultaneously.

Conclusions

A new approach is explored to study the dynamic fabrication of molecular nanoarrays with different shapes by reconstruction of supramolecular networks on HOPG. We have shown that H_3TTCA self-assembled "chicken wire" structures via hydrogen bonds at the liquid-solid interface serves as a template for the ordering of H_2Pc molecules in five new 1D nanoarrays. These five kinds of nanoarrays can be precisely turned into the $2H_2Pc@H_3TTCA$ nanoarrays by adjusting the substrate temperature. The high-resolution STM images as well as the DFT calculations reveal the preferential adsorption of the $2H_2Pc@H_3TTCA$ nanoarrays in the rearrangement H_3TTCA supramolecular networks. The results will help us gain insight into dynamic procedures of self-assembly and control molecular pattern formation on the surface.

Acknowledgments

This work was supported by the National Basic Research Program of China (Nos. 2011CB932303, 2013CB934200 and 2012CB933001). Financial supports from National Natural Science Foundation of China (Nos. 21073048, 51173031, 91127043, 21072019 and 20933008) and Beijing Jiaotong University (No. 2012RC002) are also gratefully acknowledged.

Notes and references

a CAS Key Laboratory of Standardization and Measurement for Nanotechnology, National Centre for Nanoscience and Technology, Beijing 100190, China. E-mail: zengqd@nanoctr.cn; kdeng@nanoctr.cn; wangch@nanoctr.cn

b Department of Chemistry, School of Science, Beijing Jiaotong University, Beijing, 100044, China. E-mail: wbduan@bjtu.edu.cn

c MOE Key Laboratory of Bioinorganic and Synthetic Chemistry, State Key Laboratory of Optoelectronic Materials and Technologies, School of Chemistry and Chemical Engineering, Sun Yat-Sen University, Guangzhou, 510275, China.

† Electronic Supplementary Information (ESI) available: Additional STM images. See DOI: 10.1039/b000000x/

‡ These authors contributed to this work equally.

1. J. M. Lehn, *Science*, 2002, **295**, 2400.
2. C. Joachim, J. K. Gimzewski and A. Aviram, *Nature*, 2000, **408**, 541.
3. C. Joachim and M. A. Ratner, *Proc. Natl. Acad. Sci. USA*, 2005, **102**, 8801.
4. F. Zaera, *Chem. Rev.*, 2012, **112**, 2920.
5. S. B. Lei, L. J. Wan, C. Wang and C. L. Bai, *Adv. Mater.*, 2004, **16**, 828.
6. W. Mamdouh, R. E. A. Kelly, M. D. Dong, L. N. Kantorovich and F. Besenbacher, *J. Am. Chem. Soc.*, 2008, **130**, 695.
7. X. M. Zhang, Q. D. Zeng and C. Wang, *Nanoscale*, 2013, **5**, 8269.
8. T. Kudernac, S. B. Lei, J. A. A. W. Elemans and S. De Feyter, *Chem. Soc. Rev.*, 2009, **38**, 402.
9. H. L. Liang, Y. He, Y. C. Ye, X. G. Xu, F. Cheng, W. Sun, X. Shao, Y. F. Wang, J. L. Li and K. Wu, *Coord. Chem. Rev.*, 2009, **253**, 2959.
10. Y. T. Shen, L. Guan, X. Y. Zhu, Q. D. Zeng and C. Wang, *J. Am. Chem. Soc*., 2009, **131**, 6174.
11. M. Li, K. Deng, S. B. Lei, Y. L. Yang, T. S. Wang, Y. T. Shen, C. R. Wang, Q. D. Zeng and C. Wang, *Angew.Chem., Int. Ed.*, 2008, **47**, 6717.
12. S.L. Tait, A. Langner, N. Lin, R. Chandrasekar, O. Fuhr, M. Ruben and K. Kern, *Chem. Phys. Chem.*, 2008, **9**, 2495.
13. Y. L. Yang and C. Wang, *Chem. Soc. Rev.*, 2009, **38**, 2576.
14. D. M. Cyr, B. Venkataraman and G. W. Flynn, *Chem. Mater.*, 1996, **8**, 1600.
15. S. De Feyter and F. C. De Schryver, *J. Phys. Chem. B*, 2005, **109**, 4290.
16. A. Ciesielski, C. A. Palma, M. Bonini and P. Samori, *Adv. Mater.*, 2010, **22**, 3506.
17. L. Grill, M. Dyer, L. Lafferentz, M. Persson, M. V. Peters and S. Hecht, *Nat. Nanotechnol.*, 2007, **2**, 687.
18. J. Cai, P. Ruffieux, R. Jaafar, M. Bieri, T. Braun, S. Blankenburg, M. Muoth, A. P. Seitsonen, M. Saleh, X. Feng, K. Müllen and R. Fasel, *Nature*, 2010, **466**, 470.
19. H. Y. Gao, H. Wagner, D. Y. Zhong, J. H. Franke, A. Studer and H. Fuchs, *Angew. Chem., Int. Ed.*, 2013, **52**, 4024.
20. Y. Okawa, S. K. Mandal, C. Hu, Y. Tateyama, S. Goedecker, S. Tsukamoto, T. Hasegawa, J. K. Gimzewski and M. Aono, *J. Am. Chem. Soc.*, 2011, **133**, 8227.
21. J. V. Barth, J. Weckesser, G. Trimarchi, M. Vladimirova, A. De Vita, C. Cai, H. Brune, P. Gunter and K. Kern, *J. Am. Chem. Soc.*, 2002, **124**, 7991.
22. Y. L. Huang, W. Chen, H. Li, J. Ma, J. Pflaum and A. T. S. Wee, *Small,* 2010, **6**, 70.
23. S. Clair, S. Pons, H. Brune, K. Kern and J. V. Barth, *Angew. Chem.,Int. Ed.*, 2005, **44**, 7294.
24. M. Surin, P. Samorì, A. Jouaiti, N. Kyritsakas and M.W. Hosseini, *Angew. Chem., Int. Ed.,* 2006, **46**, 245.
25. J. L. Zhang, T. C. Niu, A. T. S. Wee and W. Chen, *Phys. Chem. Chem. Phys*., 2013, **15**, 12414.
26. R. Otero, Y. Naitoh, F. Rosei, P. Jiang, P. Thostrup, A. Gourdon, E. Laegsgaard, I. Stensgaard, C. Joachim and F. Besenbacher, *Angew. Chem., Int. Ed*., 2004, **43**, 2092.
27. T. Ye, T. Takami, R. M. Wang, J. Z. Jiang and P. S. Weiss, *J. Am. Chem. Soc.,* 2006, **128**, 10984.
28. L. Xu, X. R. Miao, X. Ying and W. L. Deng, *J. Phys. Chem. C*, 2012, **116**, 1061.
29. Y. T. Shen, K. Deng, M. Li, X. M. Zhang, G. Zhou, K. Müllen, Q. D. Zeng and C. Wang, *CrystEngComm*, 2013,**15**, 5526.
30. Y. B. Li, L. H. Liu, Y. Z. Xie, X. K. Li, X. Li, X. L. Fan, K. Deng, Q. D. Zeng and C. Wang, *Phys. Chem. Chem. Phys*., 2013, **15**, 125.
31. Y. L. Huang, W. Chen and A. T. S. Wee, *J. Am. Chem. Soc*., 2011, **133**, 820.

32. Y. B. Li, K. Deng, X. K. Wu, S. B. Lei, K. Q. Zhao, Y. L. Yang, Q. D. Zeng and C. Wang, *J. Mater. Chem.*, 2010, **20**, 9100.
33. K. S. Mali, J. Adisoejoso, E. Ghijsens, I. De Cat and S. De Feyter, *Acc. Chem. Res.*, 2012, **45**, 1309.
34. L. Xu, L. Yang, L. Cao, T. Li, S. Chen, D. Zhao, S. Lei and J. Ma, *Phys. Chem. Chem. Phys.*, 2013, **15**, 11748.
35. B. Li, K. Tahara, J. Adisoejoso, W. Vanderlinden, K. S. Mali, S. De Gendt, Y. Tobe and S. De Feyter, *ACS Nano* 2013, **7**, 10764.
36. N. Kepčija, Y. Zhang, M. Kleinschrodt, J. Björk, S. Klyatskaya, F. Klappenberger, M. Ruben and J. V. Barth, *J. Phys. Chem. C.* 2013, **117**, 3987.
37. S. Vijarayaraghaven, D. Écija, W. Auwärter, S. Joshi, K. Seufert, M. Drach, D. Nieckarz, P. Szabelski, C. Aurisicchio, D. Bonifazi and J.V. Barth, *Chem. Eur. J.* 2013, **19**, 14143.
38. Y. T. Shen, K. Deng, X. M. Zhang, W. Feng, Q. D. Zeng, C. Wang and J. R. Gong, *Nano Lett.*, 2011, **11**, 3245.
39. W. R. Browne and B. L. Feringa, *Annu. Rev. Phys. Chem.*2009, **60**, 407.
40. K. Tahara,K. Inukai, J. Adisoejoso, H. Yamaga, T. Balandina, M. O. Blunt, S. De Feyter and Y. Tobe, *Angew. Chem., Int. Ed.*, 2013, **52**, 8373.
41. S. Lei, K. Tahara, F. C. De Schryver, M. Van der Auweraer, Y. Tobe and S. De Feyter, *Angew. Chem., Int. Ed.*, 2008, **120**, 3006.
42. J. Adisoejoso, K. Tahara, S. B. Lei, P. Szabelski, W. Rz˙ysko, K. Inukai, M. O. Blunt, Y. Tobe and S. De Feyter, *ACS Nano*, 2012, **4**, 897.
43. C. J. Li, Q. D. Zeng, Y. H. Liu, L. J. Wan, C. Wang, C. R. Wang and C. L. Bai, *ChemPhysChem*, 2003, **4**, 857.
44. E. Treossi, A. Liscio, X. Feng, V. Palermo, K. Müllen and P. Samori, *Small*, 2009, **5**, 112.
45. J. F. Dienstmaier, K. Mahata, H. Walch, W. M. Heckl, M. Schmittel and M. Lackinger, *Langmuir,* 2010, **26**, 10708.
46. R. Gutzler, T. Sirtl, J. F. Dienstmaier, K. Mahata, W. M. Heckl, M. Schmittel and M. Lackinger,, *J. Am. Chem. Soc.,* 2010, **132**, 5084.
47. M. O. Blunt, J. Adisoejoso, K. Tahara, K. Katayama, M. Van der Auweraer, Y. Tobe and S. De Feyter, *J. Am. Chem. Soc.,* 2013, **135**, 12068.
48. K. S. Mali, M. Georg Schwab, X Feng,K.Müllen and S. De Feyter, *Phys. Chem. Chem. Phys.,* 2013, **15**, 12495.
49. Y. N. Gong, M. Meng, D. C. Zhong, Y. L. Huang, L. Jiang and T. B. Lu, *Chem. Commun.*, 2012, **48**, 12002.
50. Y. N. Gong and T. B. Lu, *Chem. Commun.*, 2013, **49**, 7711.
51. Delley, B. *J. Chem. Phys.,* 2000, **113**, 7756.
52. J. P. Perdew and Y. Wang, *Phys. Rev. B*, 1992, **45**, 13244.
53. L. Kampschulte, T. L. Werblowsky, R. S. K. Kishore, M. Schmittel, W. M. Heckl and M. Lackinger, *J. Am. Chem. Soc.,* 2008, **130**, 8502.
54. N. T. N. Ha,T. G. Gopakumar and M. Hietschold, *J. Phys. Chem. C*, 2011, **115**, 21743.
55. S. Griessl, M. Lackinger, M. Edelwirth, M. Hietschold, W. M. Heckl, *Single Mol.,* 2002, **3**, 25.
56. X. M. Zhang, Y. T. Shen, S. Wang, Y. Y. Guo, K. Deng, C. Wang and Q. D. Zeng, *Sci. Rep.,* 2012, **2**, 742.
57. S. Lei, M. Surin, K. Tahara, J. Adisoejoso, R. Lazzaroni, Y. Tobe and S. De Feyter, *Nano Lett.,*2008, **8**, 2541.
58. F. Y. Hu, X. M. Zhang, X. C. Wang, S. Wang, H. Q. Wang, W. B. Duan, Q. D. Zeng and C. Wang, *ACS Appl. Mater. Interfaces,* 2013, **5**, 1583.
59. K. Tahara, S. Lei, J. Adisoejoso, S. De Feyter and Y. Tobe, *Chem. Commun.,*2010, **46**, 8507.
60. A. G. Slater, P. H. Beton and N. R. Champness, *Chem. Sci.,* 2011, **2**, 1440.

TOC

The phthalocyanine nanoarrays of uniform shape can be formed simply by the synergies of template effect and thermodynamic balance.